



The enhanced aerosol performance of salbutamol from dry powders containing engineered mannitol as excipient

Waseem Kaialy^a, Gary P. Martin^b, Martyn D. Ticehurst^c, Mohammed N. Momin^a, Ali Nokhodchi^{a,d,*}

^a Chemistry and Drug Delivery Group, Medway School of Pharmacy, University of Kent, ME4 4TB Kent, UK

^b King's College London, Pharmaceutical Sciences Research Group, Stamford St., Franklin-Wilkins Building, London SE1 9NH, UK

^c Pfizer Global R & D, Pharmaceutical Sciences, Sandwich, Kent CT13 9NJ, UK

^d Drug Applied Research Center and Faculty of Pharmacy, Tabriz University of Medical Sciences, Tabriz, Iran

ARTICLE INFO

Article history:

Received 20 January 2010

Received in revised form 12 March 2010

Accepted 27 March 2010

Available online 2 April 2010

Keywords:

Dry powder inhaler

Mannitol

Micromeritic

Deposition study

Crystallisation

Ratio of acetone/water

ABSTRACT

The aim of the present study was to investigate the effect of crystallising mannitol from different binary mixtures of acetone/water on the resultant physical properties and to determine the effects of any changes on *in vitro* aerosolisation performance, when the different mannitol crystals were used as a carrier in dry powder inhaler formulations containing salbutamol sulphate. Mannitol particles were crystallised under controlled conditions by dissolving the sugar in water and precipitating the sugar using binary mixtures of acetone/water in different percentages as anti-solvent media. For comparison purposes the physical properties and deposition behaviour of commercially available mannitol were also studied. SEM showed that all crystallised mannitol particles were more elongated than the commercial mannitol. Solid state studies revealed that commercial mannitol and mannitol crystallised using acetone in the presence of 10–25% v/v water as anti-solvent was β -polymorphic form whereas mannitol crystallised in the presence of a small amount of water (0–7.5%) was the α -form. All the crystallised mannitol samples showed poor flowability. Nevertheless, the powdered crystallised mannitol and commercial samples were blended with salbutamol in the ratio 67.5:1. The aerosolisation performance of the formulations containing the engineered mannitol (evaluated using Multi Stage Liquid Impinger) was considerably better than that of the commercial mannitol formulation (the fine particle fraction was increased from 15.42% to 33.07–43.99%, for the formulations containing crystallised mannitol). Generally, carriers having a high tapped density and high fraction of fine carrier particles produced a high FPF. The improvement in the DPI performance could be attributed to the presence of elongated carrier particles with smooth surfaces since these are believed to have less adhesive forces between carrier and the drug resulting in easier detachment of the drug during the inhalation.

© 2010 Elsevier B.V. All rights reserved.

1. Introduction

Since dry powder inhalers (DPIs) are pharmaceutical dosage forms which deliver drugs effectively to the respiratory tract but do not incorporate propellants as components, they have become of increasing popularity as both industry and consumers continue to appreciate the importance of 'green' issues. In addition they have a long history of successful use in the treatment of both local and systemic diseases (Timsina *et al.*, 1994).

One of the methods designed to improve DPI performance has been to use engineered drug particles or indeed, carrier particles (Maa and Prestrelski, 2000; Thompson, 1998; Chan and Chew,

2003). DPI formulations usually incorporate at least one other component, as a carrier to facilitate aerosolisation of the active agent, lactose being the most common. This sugar has been employed owing primarily to its long history of use and consequent well-established stability and safety profile. Particles of lactose can also be produced pre-determined properties such as with a smooth surface and good flow properties (Smyth and Hickey, 2005). However, the use of lactose has some disadvantages, such as its incompatibility with drugs (such as formoterol, budesonide and peptides) that have primary amine moieties (Smyth and Hickey, 2005). Furthermore, lactose can be produced with traces of their bovine source (proteins), which, therefore, carries a theoretical risk of transmissible spongiform encephalopathy (TSE) (EC Statement, 2002). Other excipients such as mannitol have been suggested as possible alternative carriers for DPI formulations (Steckel and Bolzen, 2004; Tee *et al.*, 2000).

Mannitol is an attractive alternative carrier to lactose because it does not have a reducing effect, it is less hygroscopic than some of the other sugars, gives a high sweet after-taste which could be used

* Corresponding author at: Medway School of Pharmacy, University of Kent, Pharmacy, Central Ave, Anson Building, Chatham Maritime, Kent, UK.

Tel.: +44 1634 202947; fax: +44 1634 883927.

E-mail addresses: a.nokhodchi@kent.ac.uk, phaanokhodchi@yahoo.com (A. Nokhodchi).

to confirm to the patient that a dose has been successfully administered, and it has the capacity to provide a high fine particle dose of incorporated drug upon powder aerosolisation (Saint-Lorant et al., 2007). However, the effects of engineered mannitol as a carrier on DPI performance have to date not been investigated. In this study mannitol particles were crystallised using binary combinations of acetone/water as anti-solvent. The resultant batches of crystallised mannitol powders, produced using different acetone concentrations were then tested to explore their suitability for inclusion as DPI excipients.

2. Materials and methods

2.1. Materials

Salbutamol sulphate (LB Bohle, Germany), mannitol (Fisher Scientific, UK) and acetone (Fisher Scientific, UK) were purchased from the named suppliers.

2.2. Preparation of crystallised mannitol powder by multi-solvent crystallisation

Mannitol is poorly soluble in acetone, and therefore, this organic solvent was selected as anti-solvent to recrystallise mannitol powder, using an anti-solvent precipitation technique. Mannitol (20 g) was dissolved in water (100 ml) to obtain a near-saturated solution at 70 °C under stirring conditions. A series of anti-solvent media with different ratios of acetone:water (100:0, 95:5, 92.5:7.5, 90:10, 85:15, 80:20 and 75:25 ml) were prepared (the total volume of each combination being 100 ml). These anti-solvent media were heated to 30 ± 1 °C, and the temperature was maintained constant for 10 min. After temperature equilibration, 20 ml of the saturated solution of mannitol was added to 100 ml of the anti-solvent medium at a constant rate of 2.5 ml/min under constant stirring condition. After adding the total volume of saturated mannitol, all the beakers containing the crystallised mannitol were removed from the heat, covered tightly with parafilm, and stored unstirred at room temperature (22 ± 2 °C) for 24 h. The suspensions were then filtered under vacuum through a filtration unit containing a Whatman filter paper (<0.45 µm). Crystallised mannitol samples obtained using the lower ratios of acetone:water (80:20 and 75:25) (high amounts of water) were stored for 48 h before filtering due to the low yield obtained after 24 h. The harvested crystallised mannitol samples were dried for 24 h in an oven at 75 °C before being transferred to a glass vial, which was, subsequently, sealed and the samples retained for further investigation.

2.3. Particle size analysis

Particle size analysis was conducted on an aerosolised dry sample using a Sympatec (Clausthal-Zellerfeld, Germany) laser diffraction particle size analyser. The volume mean diameter (VMD), and other particle size parameters corresponding to the size of the 10th, 50th and 90th percentile of particles ($D_{10\%}$, $D_{50\%}$ and $D_{90\%}$) were calculated automatically using the software provided. Approximately 2–3 g of the sample was transferred into the funnel of the VIBRI. The sample container was cautiously tapped against the funnel to ensure all the contents emptied. A test reference measurement was performed with the HELOS sensor using WINDOX software followed by a standard measurement. This was to ensure the material was flowing through the vibrating chute into the groove of the rotary table. The results are the mean and standard deviation of three to five determinations.

2.4. Powder flow measurement

The bulk and tapped densities were measured. Carr's Index and Hausner ratio were calculated and employed as an indication of flowability of the mannitol samples. The powder was filled into a 5 ml measuring cylinder and after recording the volume (bulk volume) the cylinder was tapped 100 times under ambient conditions (20 °C, 50% RH) and the new volume was recorded (tapped volume). The preliminary results showed that the use of 100 taps was sufficient to attain the minimum volume of the powders under study. Carr's Index and Hausner ratio were calculated using the following equations (Carr, 1965a,b).

$$\text{Carr's Index} = \left[\frac{\text{Tapped density} - \text{Bulk density}}{\text{Tapped density}} \right] \times 100 \quad (1)$$

$$\text{Hausner ratio} = \frac{\text{Tapped density}}{\text{Bulk density}} \quad (2)$$

Carr's Index values of less than 25% and Hausner ratio values less than 1.25 indicate acceptable flow properties.

2.5. True density measurement

The true density of all mannitol samples was measured using an ultrapycnometer 1000 (Quantachrom, USA) and helium gas according to the manufacturer's guidelines. The true density was taken as the mean of three determinations.

2.6. Fourier transition infrared spectroscopy (FT-IR)

FT-IR spectra were used to investigate any possible changes in crystallised mannitol that may have occurred at the molecular level during the crystallisation or drying processes. These spectra were recorded using ATR, FT-IR (PerkinElmer, USA) equipment for the different crystallised mannitol crystals. The scanning range was 450–4000 cm^{-1} and the resolution was 1 cm^{-1} .

2.7. Scanning electron microscope (SEM)

Electron micrographs of the original and crystallised mannitol samples were obtained using a scanning electron microscope (Philips XL 20, Eindhoven, Netherlands) operating at 15 kV. The specimens were mounted on a metal stub with double-sided adhesive tape and coated under vacuum with gold in an argon atmosphere prior to observation.

2.8. Different scanning calorimetry (DSC)

A differential scanning calorimeter (DSC7, Mettler Toledo, Switzerland) was used to measure the enthalpy and melting point of the different mannitol samples. The equipment was calibrated using indium and zinc. Samples weighing between 4 and 5 mg were crimped and sealed in aluminium DSC pans with pin-hole lids. Samples were heated from 25 to 300 °C at a scanning rate of 10 °C/min under nitrogen gas. The melting points and enthalpies of fusion were calculated using the supplied software (Mettler, Switzerland).

2.9. Shape factors determination

A micro-spatula was used to sample about 20 mg of powder, and a microscope slid and the powder was gently finger-tapped above the microscope slide. The microscope slide was then also manually tapped to remove accumulated powder until very thin powder dust was homogeneously scattered over the slide. Particle size and shape were assessed using image analysis software (designed in-house at King's College London) installed on an Archimedes computer,

which was attached to an optical microscope (Nikon Labophot, Tokyo, Japan) via a miniature video camera. 100 particles were selected and measured in each sample and the surface-volume mean diameter, Feret diameter, elongation ratio, and roundness were calculated. Roundness and elongation ratio were calculated using Eqs. (3) and (4), respectively

$$\text{Roundness} = \frac{(\text{perimeter})^2}{4 \times \pi \times \text{area}} \quad (3)$$

$$\text{Elongation ratio} = \frac{\text{Maximum Feret diameter}}{\text{Minimum Feret diameter}} \quad (4)$$

Particle size was calculated as the diameter of an equivalent sphere that produces a projected image of the same area to the measured particle. Elongation ratio and roundness were used as the two-dimensional shape descriptors to quantify the mannitol particle shape.

2.10. Sieving

The crystallised mannitol samples were sieved to separate the 63–90 μm fraction by pouring the powder onto the top of 90 μm sieve which was placed above a 63 μm sieve. The sieve shaker (Retsch® GmbH Test Sieve, Germany) was then operated for 15 min. After the sieving process was complete, the particles retained on the 63 μm sieve were collected and stored in sealed glass vial until required for further investigation. The commercial mannitol was also sieved under the same conditions.

2.11. In vitro formulation assessment

2.11.1. Blending mannitol with salbutamol sulphate

Each crystallised sieved (63–90 μm) mannitol sample was geometrically blended with salbutamol sulphate (SS) to provide a final ratio (sugar:drug) of 67.5:1 w/w, which is in accordance with the ratio used in commercial Ventolin™ Rotacaps™ (GSK) formulations. The blending was carried out using a Turbula mixer (Maschinen fabrik, Basel, Switzerland) at a constant speed of 136 rpm for 30 min. All the formulation blends were then stored in tightly sealed glass vials.

2.11.2. Determination of the homogeneity of the formulation mixtures

After blending the drug with carrier, the homogeneity of the drug content in each of the powder formulations was examined by taking a minimum of five randomly selected samples from different positions within the blend. Each sample weighing 33 ± 1.5 mg (this was the amount of the powder mixture to be introduced into each capsule) was dissolved in 100 ml water contained in a volumetric flask. The amount of the active drug (salbutamol sulphate) in each powder formulation was determined using a high performance liquid chromatography (HPLC) method, as described below. The degree of uniformity or (homogeneity) was expressed in terms of the percentage coefficient of variation (CV %) and a percentage CV less than 6% was taken as an indication of acceptable uniformity.

2.11.3. Capsule filling

Each formulation was filled manually in a hard gelatine capsule (size 3) with 33.0 ± 1.5 mg so that each capsule contained 481 ± 2 μg salbutamol sulphate which was similar to the unit dose used in a Ventolin Rotacap®.

2.11.4. Dry powder inhaler performance characterisation

The *in vitro* powder pulmonary deposition behaviour of salbutamol sulphate from each formulation was assessed using an Aerolizer® (the device was supplied by Vectura, UK and originated

by Novartis, Switzerland) with a Multi Stage Liquid Impinger (MSLI) equipped with an accurately fitted USP induction port (Copley Scientific, Nottingham, UK). Prior to testing, 20 ml of distilled water was introduced to the stages 1–4 of the MSLI in order to make the collection surfaces wet. The inhaler containing a filled capsule was fitted in a rubber mouthpiece adaptor and then attached to the impinger induction port (IP). A filter paper (Whatman®; pore size, <70 μm) was introduced in the stage 5 of the impinger. The flow rate was set at 92 l/min (a flow rate established in a previous study as being realistically achieved by patients using such a device Srichana et al., 1998). Then the capsule was pierced and the encapsulated powder aerosolised. Ten actuations (i.e. 10 capsules) of each powder were effected and the aerosolised contents delivered consecutively to the MSLI at a pressure of 4 kPa.

After 10 actuations, the water on each stage was recovered and then the stages of the MSLI were thoroughly washed with additional distilled water several times to collect all the powder deposited (the final volume of water used to wash each stage was 100 ml). The powder deposited on the induction port was also collected by washing with distilled water and the volume adjusted to 100 ml. The 10 individual inhalers which were used in each study with their mouthpiece adapters were also washed thoroughly and the volume of solution also adjusted to 100 ml, in preparation for assay. The integral filter paper which was introduced to the stage five of the impinger to ensure that the drug deposited as the smallest particles was also included.

The amount of drug in each sample was determined using an HPLC method, as described below. The amount of salbutamol sulphate deposited on the inhaler and mouthpiece adaptor, induction port, and each individual impaction stage of the MSLI was quantified using the calibration curve. Each formulation was tested three times to obtain a valid comparison of the deposition data. Several parameters were employed to characterise the resultant deposition profiles of salbutamol sulphate from each formulation. These were: the recovered dose (RD), which is the sum of the weights of drug (μg) recovered from inhaler device with its fitted mouthpiece adaptor, induction port, and all stages of the impactor and the emitted dose (ED), which is the amount of drug delivered from the inhaler device, which is collected in the induction port and all stages of the impactor (i.e. total RD except for the inhaler device with mouthpiece adaptor). In order to calculate FPF a plot was drawn of the cumulative mass of powder less than the stated size of MSLI stages 1–4 as a percentage of the emitted dose from the impactor against the log value of the effective cut-off diameter. The effective cut-off diameter is the new cut-off diameter of each stage of the MSLI when it is operated at a different flow rate from 60 l/min. In order to calculate the effective cut-off diameter of each individual stage of the MSLI at flow rate of 92 l/min, the following equation was employed (USP, 2003):

$$D_{50,Q} = D_{50,Q_n} \left(\frac{Q_n}{Q} \right)^{1/2} \quad (5)$$

where $D_{50,Q}$ is the cut-off diameter at a flow rate of Q , n refers to nominal values obtained. $Q_n = 60$ (which is as following for MSLI stages 1–4, respectively: 13.0, 6.8, 3.1, and 1.7 μm). Q is the operating flow rate during the test (which is 92 l/min).

The FPF was calculated from that plot as the fraction of powder emitted from the inhaler with an aerodynamic diameter ≤ 5 μm . In order to calculate the experimental the mass median aerodynamic diameter (MMAD), the cumulative percentage of drug mass less than the stated aerodynamic diameter of MSLI stages from 1 to 4 was calculated and plotted against the effective cut-off diameter on log probability paper taking cumulative amounts less than MSLI stage 1 as 100% (USP, 2003). MMAD is the particle size at which the line crossed the 50% mark (as the 50th percentile of the aerodynamic particle size distribution by mass). The same plot was used

to calculate the geometric standard deviation as the square root of the ratio of particle size at the 84.13th percentile to the 15.87th percentile.

The percent total recovery (% recovery) was calculated as the ratio of the RD to the theoretical dose ($481 \pm 22 \mu\text{g}$). The theoretical dose ($481 \pm 22 \mu\text{g}$) was taken as being equivalent to the dose contained in the powder weight of formulation filled in each capsule ($33 \pm 1.5 \text{ mg}$). The percent emission was the ratio of the ED to RD. Impaction loss was defined as the amount of drug deposited on the induction port and stage 1 of the MSLI as a percentage of the recovered dose. All assessments were performed in triplicate.

2.11.5. HPLC quantification of salbutamol sulphate

Salbutamol sulphate was analysed using a HPLC method (Waters, USA). A mixture of methanol and 0.25% (w/v) 1-heptane sulphonic acid sodium salt (45:55 v/v) was used as mobile phase. The flow rate of mobile phase was 2 ml/min and the assay wavelength was 200 nm. The HPLC system consisted of a pump (CM4000 Multiple Solvent Delivery System, LDC Analytical Inc., FL, USA), a multiple wavelength UV detector (SpectroMonitor 3100, LDC Analytical Inc., FL, USA) and a 25 cm \times 4.6 mm i.d. column packed with 5 μm Novapack C18 (Waters, Milford, MA, USA). The retention time for salbutamol sulphate was 3.2 min and the limits of detection and quantification were 0.16 and 0.49 $\mu\text{g}/\text{ml}$, respectively.

3. Results and discussion

3.1. Crystallisation procedure

During the crystallisation process the induction time, i.e. the time taken for crystals to appear after initiation addition of the anti-solvent, was dependent on the ratio of acetone/water employed. Not surprisingly, due to the higher solubility of mannitol in water, the induction time was increased as the amount of water in binary mixtures of acetone–water increased. When acetone was

used alone the crystallisation was initiated immediately. However regardless of the speed of crystal formation (different induction times), the amount of recovered mannitol was high and it varied between 71.62% and 100% (Table 1). It was also noted that the particles crystallised from 100 ml acetone were fluffy in appearance when isolated but this property diminished as the water content of the anti-solvent was increased. These visual observations were supported by the bulk and tapped density data (Table 1).

3.2. Densities and flow properties

True density values of commercial mannitol and all the crystallised mannitol samples are shown in Table 1. The true density of commercial mannitol was 1.516 g/cm³ which was similar to the previously reported value (1.51 g/cm³) (Rowe et al., 2003). True density measurements of the crystallised mannitol samples ranged between 1.46 and 1.53 g/cm³. ANOVA (one way analysis of variance) test showed that the presence of water in crystallisation medium affected the true density of the resultant mannitol crystals ($P < 0.05$).

The tapped density of a powder influences the aerosolisation performance of the powder, the latter being improved as tapped density is lowered (Bosquillon et al., 2001). The tapped density of commercial mannitol was 0.63 g/cm³, while all crystallised mannitol powders exhibited a lower tapped density, within in the range between 0.17 and 0.40 g/cm³ (Table 1). Indeed a linear relationship was obtained between the water content (%) of the anti-solvent and the resultant tapped density ($r^2 = 0.933$). This linear relationship could be used to predict the tapped density of mannitol particles crystallised from binary mixtures of acetone/water. A similar relationship existed between percentage water content of the anti-solvent used in the crystallisation of mannitol and bulk density with $r^2 = 0.828$.

CI for commercial mannitol was $14.17 \pm 0.79\%$, which was significantly lower than the values obtained for the crystallised mannitol

Table 1

Percentage yield, true density, bulk density, tapped density, Carr's Index, and Hausner ratio of commercial mannitol and crystallised mannitol, obtained using different anti-solvent media (values are the mean \pm standard deviations, $n = 3$).

Sample	Yield %	True density (g/cm ³)	Bulk density (g/cm ³)	Tapped density (g/cm ³)	Carr's Index (%)	Hausner ratio
Commercial mannitol	–	1.52 \pm 0.00	0.54 \pm 0.01	0.63 \pm 0.01	14.17 \pm 0.79	1.16 \pm 0.01
Mannitol crystallised using: acetone:water (100:0)	84.75	1.51 \pm 0.01	0.11 \pm 0.00	0.17 \pm 0.01	36.00 \pm 5.29	1.57 \pm 0.12
Acetone:water (97.5:2.5)	88.00	1.53 \pm 0.00	0.14 \pm 0.01	0.20 \pm 0.01	32.67 \pm 1.15	1.48 \pm 0.02
Acetone:water (95:5)	99.50	1.51 \pm 0.01	0.20 \pm 0.03	0.27 \pm 0.01	25.67 \pm 7.23	1.35 \pm 0.14
Acetone:water (92.5:7.5)	97.50	1.53 \pm 0.01	0.14 \pm 0.01	0.23 \pm 0.01	38.00 \pm 1.73	1.61 \pm 0.04
Acetone:water (90:10)	71.62	1.53 \pm 0.01	0.15 \pm 0.01	0.24 \pm 0.00	36.33 \pm 3.21	1.57 \pm 0.08
Acetone:water (85:15)	82.91	1.47 \pm 0.01	0.21 \pm 0.01	0.31 \pm 0.03	32.67 \pm 4.16	1.49 \pm 0.09
Acetone:water (80:20)	101.25	1.52 \pm 0.01	0.24 \pm 0.04	0.35 \pm 0.01	31.67 \pm 7.57	1.47 \pm 0.15
Acetone:water (75:25)	102.50	1.46 \pm 0.00	0.26 \pm 0.00	0.40 \pm 0.00	34.67 \pm 1.15	1.53 \pm 0.03

Table 2

Volume mean diameter, span, particle size distribution expressed as $D_{10\%}$, $D_{50\%}$, $D_{90\%}$, and percentage of particles less than 10.50 μm for commercial mannitol and crystallised mannitol samples (values are the mean \pm standard deviations, $n = 3$).

	% < 10.50 (μm)	$D_{10\%}$ (μm)	$D_{50\%}$ (μm)	$D_{90\%}$ (μm)	VMD (μm)	Span	S_v : surface area based on volume distribution (m ² /cm ³)
Commercial mannitol	0.00 \pm 0.00	66.14 \pm 0.69	106.73 \pm 0.78	149.46 \pm 0.89	107.44 \pm 0.67	0.77 \pm 0.01	0.06 \pm 0.00
Mannitol crystallised using: acetone:water (100:0)	17.42 \pm 4.28	5.51 \pm 1.59	55.80 \pm 9.70	102.34 \pm 6.34	54.47 \pm 7.23	1.79 \pm 0.16	0.52 \pm 0.13
Acetone:water (97.5:2.5)	20.51 \pm 2.36	4.94 \pm 0.69	48.21 \pm 7.72	119.10 \pm 24.87	55.34 \pm 9.92	2.05 \pm 0.11	0.56 \pm 0.06
Acetone:water (95:5)	23.30 \pm 7.10	4.73 \pm 1.75	38.06 \pm 15.32	94.49 \pm 8.92	44.36 \pm 8.69	2.06 \pm 0.25	0.65 \pm 0.15
Acetone:water (92.5:7.5)	20.55 \pm 7.27	6.07 \pm 2.71	45.21 \pm 17.82	98.93 \pm 24.48	49.52 \pm 15.49	1.91 \pm 0.17	0.53 \pm 0.16
Acetone:water (90:10)	29.17 \pm 4.46	3.47 \pm 0.58	70.44 \pm 32.39	150.26 \pm 4.65	72.57 \pm 8.10	2.04 \pm 0.19	0.69 \pm 0.11
Acetone:water (85:15)	2.90 \pm 0.33	45.16 \pm 3.00	81.21 \pm 2.72	127.59 \pm 3.61	83.17 \pm 2.85	0.99 \pm 0.04	0.21 \pm 0.01
Acetone:water (80:20)	19.49 \pm 5.70	5.05 \pm 0.98	72.32 \pm 6.50	117.03 \pm 4.74	67.90 \pm 7.50	1.66 \pm 0.13	0.40 \pm 0.09
Acetone:water (75:25)	0.00 \pm 0.00	60.25 \pm 1.43	87.94 \pm 1.60	125.07 \pm 5.67	90.62 \pm 1.91	0.71 \pm 0.06	0.07 \pm 0.00

samples, which varied between $25.67 \pm 7.23\%$ and $38.00 \pm 1.73\%$ (Table 1). These data indicate that the crystallised mannitol samples would be expected to display greater compressibility but less flowability in comparison to the commercial mannitol sample. This might be attributable in part to the presence of needle-shaped mannitol particles in the crystallised samples. CI was the same for all crystallised mannitol samples (ANOVA; $P > 0.05$). A similar conclusion could be drawn regarding the flowability of the crystallised powders in comparison to commercial mannitol, when Hausner ratio values were considered (Table 1).

3.3. Particle size analysis

The commercial mannitol sample possessed the highest VMD ($107.44 \mu\text{m}$), while VMDs of all the crystallised mannitol samples (ranging from 44.36 to $90.62 \mu\text{m}$) were significantly smaller (Table 2). Generally, the higher the water content of the anti-solvent, the higher VMD of the resultant crystallised mannitol. The span value, a measure of particle size distribution, obtained for commercial mannitol sample (0.77 ± 0.01) was lower than the span values reported for some of the crystallised samples. Therefore, nearly all of the crystallised samples showed a wider particle size distribution (high polydispersity) in comparison with commercial mannitol. It was assumed that loose aggregates of mannitol particles during size measurement were disrupted to produce fine needle-like particles resulting in increased polydispersity within the sample.

Despite all the mannitol samples being sieved in the same way, no fine particles less than $10.50 \mu\text{m}$ were found in the commercial mannitol sample, while a high amount of fines (up to 29.17%) was found in the crystallised mannitol samples (Table 2). The fines content of the mannitol sample crystallised using acetone:water with the ratio of 90:10 was especially high. The presence of such fines might be expected to affect aerosolisation performance (Islam et al., 2004).

The surface area on the basis of particle volume (S_v) for untreated mannitol was $0.06 \text{ m}^2/\text{cm}^3$, while all recrystallised mannitol samples showed higher S_v values compared to commercial mannitol (ranging from 0.07 to $0.69 \text{ m}^2/\text{cm}^3$ (Table 2)) which could be attributed to the needle shape of crystallised mannitol particles.

The size distribution analysis of salbutamol sulphate indicated that the drug had a mono-modal distribution with a volume mean diameter (VMD) of $1.86 \pm 0.16 \mu\text{m}$, $D_{50\%}$ of $1.66 \pm 0.06 \mu\text{m}$, and 90% of the particles less than $3.14 \pm 0.31 \mu\text{m}$. Since a majority of the particles was less than $5 \mu\text{m}$, then the drug might be considered to have an optimal size for pulmonary delivery by DPI (Pritchard, 2001).

3.4. Scanning electron microscopy

Commercial mannitol contained large rounded particles, having irregular surfaces with some adherent fine micro-particles apparent (Fig. 1). As indicated above the crystallised samples contained primarily elongated needle-shaped particles (this is likely to be

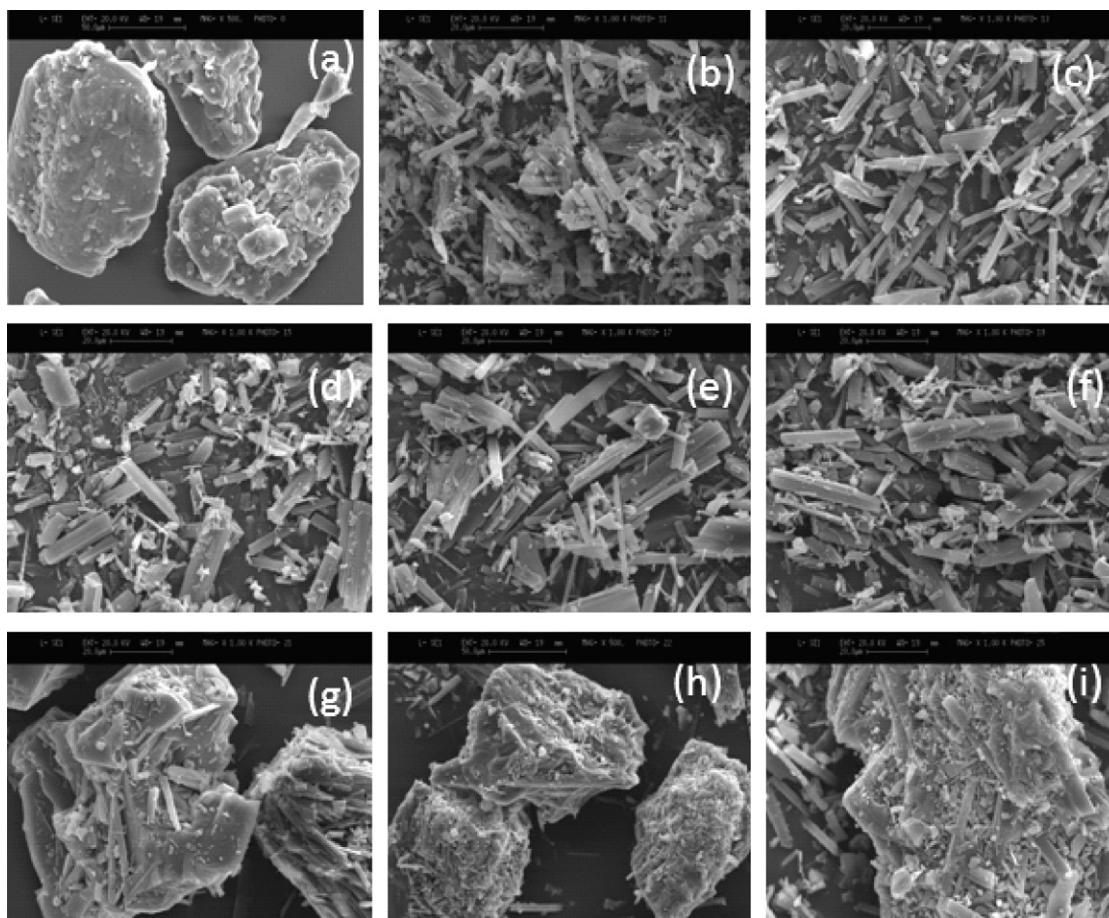


Fig. 1. SEM images of (a) commercial mannitol, mannitol crystallised using anti-solvent containing: (b) acetone 100%, (c) acetone:water 97.5:2.5%, (d) acetone:water 95:5%, (e) acetone:water 92.5:7.5%, (f) acetone:water 90:10%, (g) acetone:water 85:15%, (h) acetone:water 80:20%, (i) acetone:water 75:25% v/v (magnification for all samples is $1000\times$).

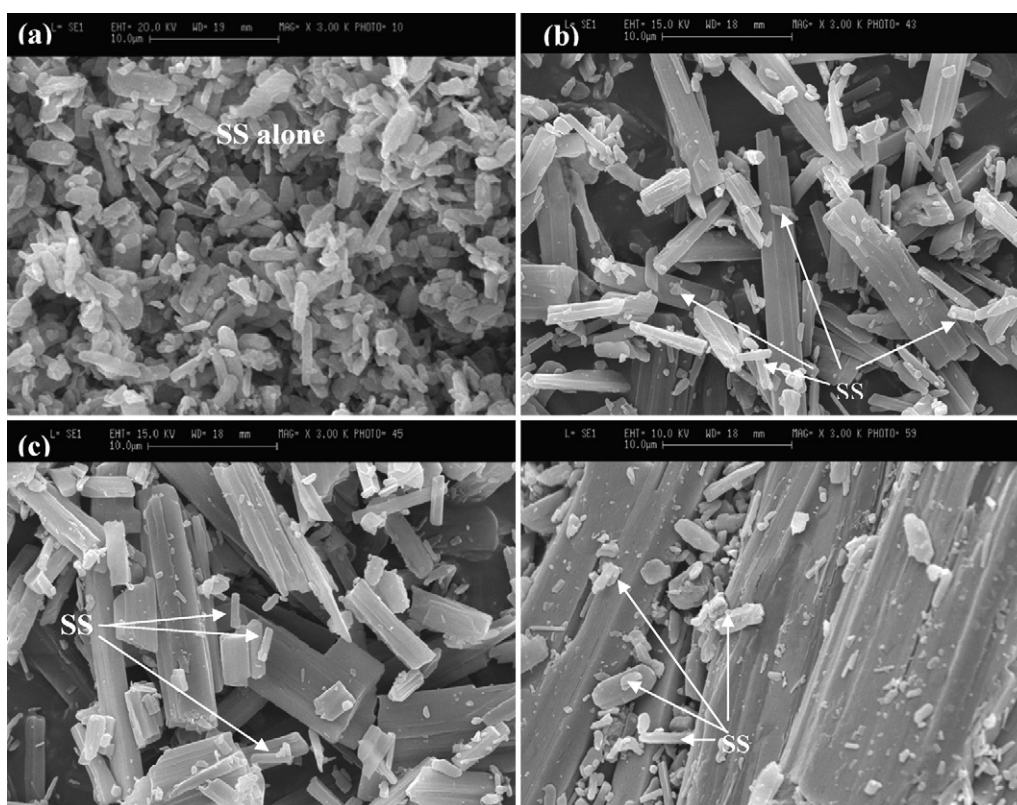


Fig. 2. SEM images of (a) salbutamol sulphate and different mannitol–salbutamol sulphate formulation blends, the mannitol crystallised using: (b) 100% acetone, (c) acetone:water, 97.5:2.5%, or (d) acetone:water, 75:25% as anti-solvent (magnification for all samples was 3000 \times).

the main reason for poor flowability of crystallised mannitol samples and the estimated particle sizes were in good agreement with the particle size distribution obtained by laser diffraction (Table 2).

Comparing the SEM images of various mannitol samples crystallised using different ratios of acetone/water showed that increasing the percentage of water used in the anti-solvent during the crystallisation process resulted in the generation of thicker crystals. Mannitol samples crystallised using acetone containing 15%, 20% and 25% water showed some particle agglomeration (Fig. 1g–i). The difference in shape is likely to be due to the accelerated growth of the longest axis during the crystallisation procedure at the expense of the crystal width and thickness, which occurs at the higher acetone ratios. The more water used in the anti-solvent, the less the elongation of the resultant mannitol crystals. In the formulation blends, salbutamol sulphate was apparent, adhering to the surface of the mannitol carrier, suggesting the formation of interactive mixtures (Fig. 2). SEM images of salbutamol sulphate-carrier blends show that in addition to adherent fine salbutamol particles, some fine carrier particles were also attached to the car-

rier surfaces (salbutamol sulphate particles could be recognised by their rod shape).

3.5. Particle shape analysis

Surface-volume mean diameter, roundness, and elongation ratio were measured for the commercial mannitol sample and all the crystallised mannitol samples (Table 3). A linear relationship ($r^2=0.88$) existed between the amount of water used in the anti-solvent for mannitol crystallisation and the logarithm of surface-volume mean diameter of the crystallised particles (Fig. 3), with an increased water content of the anti-solvent producing a larger particle. On the other hand, the roundness and elongation ratio of the crystallised mannitol samples was found to decrease as a function of the increased percentage water used in the anti-solvent (Fig. 3). It can be concluded that, the water content of the anti-solvent used to crystallise mannitol had a considerable effect on the shape factors of the resultant mannitol particles and all the crystallised samples were more elongated and further from sphericity in comparison to

Table 3

Surface-volume diameter, roundness, and elongation ratio for commercial mannitol particles, and crystallised mannitol which was assessed using optical image analysis (values are the mean standard deviations, $n=100$).

Carrier (63–90 μm)	Surface-volume diameter (μm)	Roundness	Elongation ratio
Commercial mannitol	143.74 \pm 1.46	1.47 \pm 1.01	1.62 \pm 0.43
Mannitol crystallised using: acetone:water (100:0)	38.89 \pm 1.46	4.47 \pm 2.03	4.83 \pm 1.83
Acetone:water (97.5:2.5)	36.10 \pm 1.45	4.26 \pm 2.17	4.56 \pm 4.56
Acetone:water (95:5)	39.69 \pm 1.38	3.78 \pm 1.38	4.57 \pm 1.71
Acetone:water (92.5:7.5)	42.37 \pm 1.50	3.64 \pm 1.36	4.32 \pm 1.56
Acetone:water (90:10)	52.31 \pm 1.48	3.09 \pm 1.39	3.05 \pm 1.59
Acetone:water (85:15)	59.91 \pm 1.56	2.72 \pm 1.28	3.06 \pm 1.58
Acetone:water (80:20)	160.05 \pm 2.08	2.83 \pm 1.66	2.66 \pm 1.46
Acetone:water (75:25)	293.14 \pm 2.39	2.90 \pm 1.78	3.33 \pm 2.21

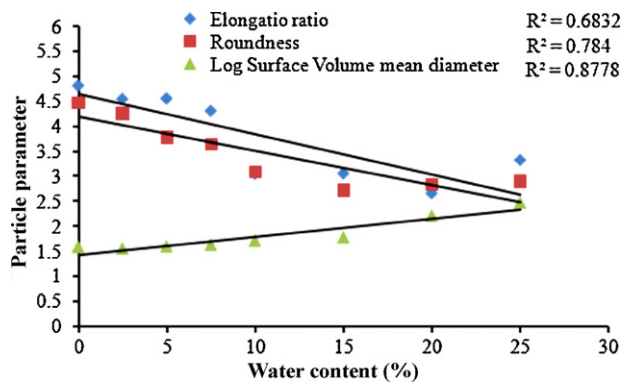


Fig. 3. Linear relationship between surface-volume mean diameter, elongation ratio, or roundness of mannitol crystals and the percentage water used in the anti-solvent to crystallise mannitol.

the commercial sample. Moreover, the water content of the acetone/water mixtures could be controlled so as to prepare crystallised mannitol particle with pre-determined shape in terms of surface-volume mean diameter, roundness, and elongation ratio (Fig. 3).

3.6. Solid state characterisation

3.6.1. Different scanning calorimetry (DSC)

The DSC thermograms of the commercial mannitol contained one endothermic peak at about 167°C which corresponds to the melting point of mannitol (figure not shown). The thermograms of the crystallised mannitol samples were similar to that obtained for the sample of commercial mannitol. A comparison of the melting and enthalpy data for each of the mannitol samples indicated that there was no difference between data, suggesting that the same polymorphic forms were obtained under all crystallisation conditions (enthalpy for untreated mannitol was 315.29 ± 10.69 J/g and for all recrystallised samples was between 305.64 ± 0.60 and 320.49 ± 1.75 J/g).

3.6.2. Fourier transition infrared (FT-IR)

Mannitol is reported to have at least three different polymorphic forms: α , β and δ (Campbell et al., 2002). These polymorphs are reported to have different FT-IR spectra in the finger print region between 2500 and 3700 cm^{-1} (Yoshinari et al., 2002; Burger et al., 2000) and 800–1400 cm^{-1} . Structural features of polymorphs β and δ cause these differences in the FT-IR spectrum and can be ascribed to variations in O–H or C–H stretching. Comparing all bands present from 2800 to 3600 cm^{-1} showed that there was no apparent difference between different mannitol samples (Fig. 4). Other important areas of the IR spectrum that can be used to identify different polymorphs are in the wavelength ranges 1200–1400, 650–800 and 1100–1150 cm^{-1} . To investigate whether there were differences in these regions, the spectra were expanded (Fig. 4II). It can be seen that commercial mannitol showed three distinctive peaks at 1209, 959 and 929 cm^{-1} . These characteristic peaks are accounted for by the presence of the β -form and are in agreement with previous studies (Burger et al., 2000; Walter-Levy, 1968). The same distinctive peaks could be observed for the mannitol crystallised using acetone/water anti-solvents containing 10%, 15%, 20%, and 25% v/v water. However, samples prepared using smaller amounts of water (0%, 2.5%, 5%, and 7.5%) did not show these peaks, but showed two other distinctive peaks at 1195 cm^{-1} which correspond to α -mannitol (Burger et al., 2000; Walter-Levy, 1968). As a conclusion, FT-IR spectra indicated that commercial mannitol and crystallised mannitol prepared using water content from 15% to 25% results in

the appearance of the β -form, while mannitol samples crystallised from acetone/water containing less than 10% water appeared to results in the α -form. However, these different polymorphic forms could not be identified from the DSC thermograms of the crystalline powders.

3.7. Aerosolisation performance assessment

3.7.1. Content uniformity test

The mean salbutamol sulphate content of the commercial mannitol formulation blend was 450.67 ± 7.92 μg , while the average salbutamol sulphate content of all the crystallised mannitol samples was in the range between 439.60 ± 23.43 and 489.71 ± 31.32 μg (Table 4). The acceptable dose range for dry powder inhalers is the nominal dose ±10% which for these formulation blends provides a range from 432.90 to 529.10 μg . All formulation blends were within this range (Table 4). Following mixing, the coefficient of variation for the drug content of the commercial mannitol sample was found to be lower (1.76%) than the coefficient of variation for the crystallised mannitol formulations (ranging from 3.39% to 17.40%). Similar results were reported when needle-shaped lactose was blended with needled-shaped salbutamol sulphate (Larhrib et al., 2003).

3.7.2. Deposition studies

The deposition profiles of drug produced after aerosolisation of the blends containing crystallised mannitol were significantly different to that obtained when the formulation containing commercial mannitol was aerosolised (Table 5). The RD of the crystallised mannitol formulations was between 395.21 μg (mannitol recrystallised using acetone containing 15% water) and 458.73 μg (mannitol crystallised using acetone containing 5% water). This range was considerably higher than the RD of salbutamol from the formulation containing commercial mannitol, where the RD was 381 ± 8.27 μg . The percentage recovery of salbutamol sulphate ranged between 82.16 ± 19.84% and 95.37 ± 15.40% from formulations containing crystallised mannitol and these values were all higher than the percentage recovery of drug from the formulation containing commercial mannitol (79.32 ± 1.72%). This indicates that the use of crystallised mannitol rather than the commercial grade sugar within the blend might be expected to produce a better aerosolisation of the drug. The RD from all formulations containing crystallised mannitol was within the previously reported acceptable range of 75–125% (Byron et al., 1994).

Similar results were obtained for ED of drug which when using crystallised mannitol in the powder blends was between 373.21 ± 101.27 μg and 433.32 ± 69.07 μg . Again, the ED from formulations containing crystallised mannitol was higher than from the blend containing commercial grade mannitol (367.30 ± 8.81 μg). The difference in water content of the anti-solvent did not significantly affect the RD and the ED of the drug from powders containing crystallised mannitol (ANOVA; $P > 0.05$). The highest RD (458.73 ± 74.07 μg) and ED (433.32 ± 69.07 μg) occurred after aerosolisation of the formulation containing mannitol crystallised using an acetone:water (95:5) as anti-solvent (Table 5).

The emission values of drug from the aerosolised powders containing crystallised mannitol were all between 92.93 ± 1.56% and 94.94 ± 1.14%, indicating that only about 5–7% of the drug was retained in the inhaler device including mouthpiece adaptor (Table 5). There was no significant difference between the emissions of drug from the formulations containing crystallised mannitol ($P > 0.05$), whereas the percentage emission from the formulation containing commercial mannitol blend (96.28 ± 0.22) was slightly higher than from the other blends. This might be attributable to the better flowability of the commercial manni-

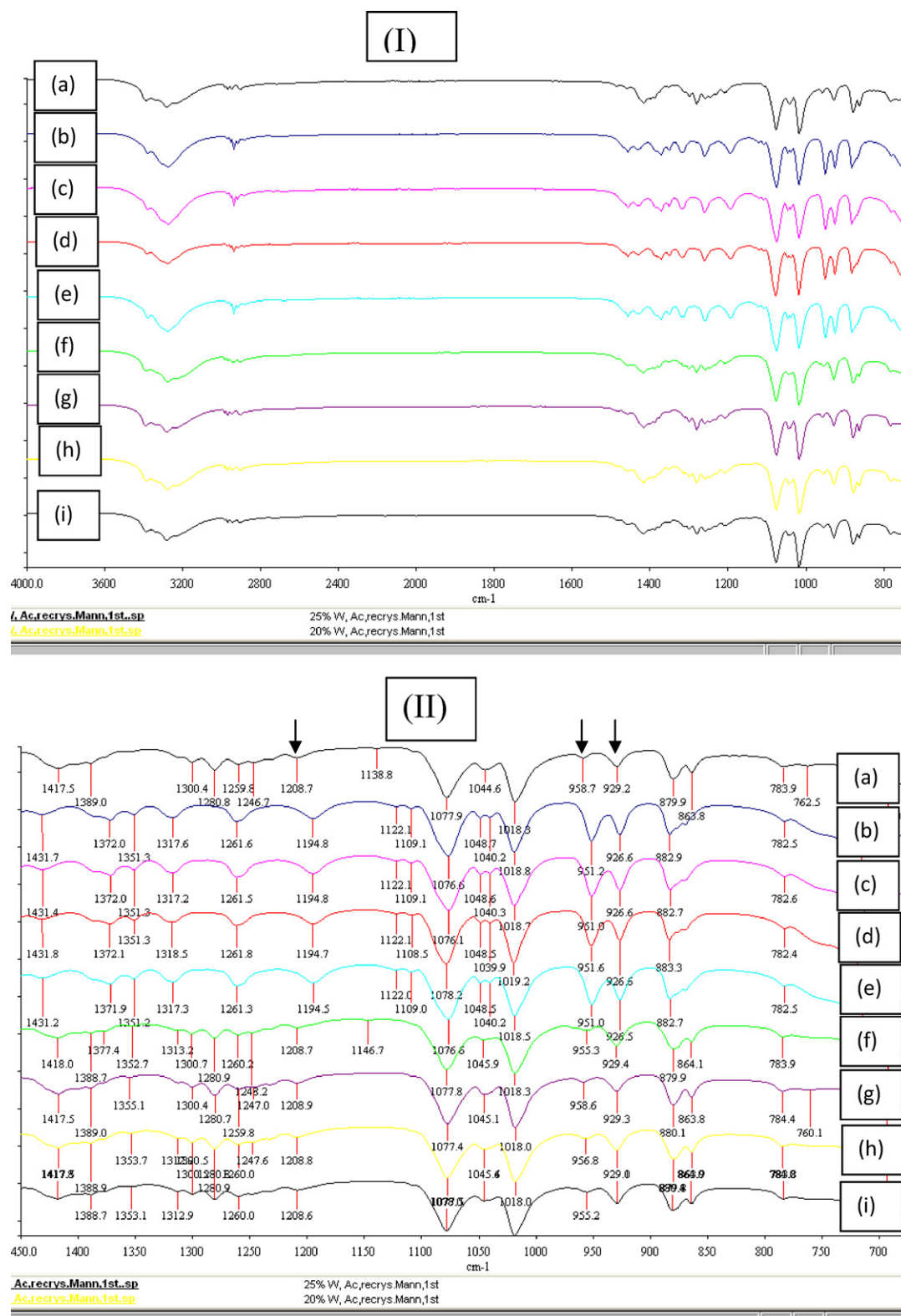


Fig. 4. FT-IR spectra of: (a) commercial mannitol, mannitol recrystallised from media using different anti-solvents: (b) acetone 100%, (c) acetone:water 97.5:2.5%, (d) acetone:water 95:5%, (e) acetone:water 92.5:7.5%, (f) acetone:water 90:10%, (g) acetone:water 85:15%, (h) acetone:water 80:20%, (i) acetone:water 75:25%.

tol in comparison to the crystallised mannitol (see CI reported in Table 1). However, the incorporation of crystallised mannitol in the formulation with salbutamol sulphate did therefore result in marginally higher amounts of drug depositing in the inhaler and on the mouthpiece adaptor (Table 6).

It has been reported that better aerosolisation performance was associated with better flow properties for spray dried DPI formulations (Rabbani and Seville, 2005). However, in this study the samples containing crystallised mannitol exhibited a better aerosolisation performance despite the poorer flow properties

Table 4

The percentage uniformity and the coefficient of variation (CV) in salbutamol sulphate content obtained from the formulation containing commercial mannitol and batches containing crystallised mannitol using anti-solvents containing different acetone:water ratios (values are the mean \pm standard deviations, $n = 5$).

Formulation	% Uniformity	Drug content (μg)	% CV
Commercial mannitol	93.69 \pm 1.65	450.67 \pm 7.92	1.76
Mannitol crystallised using: acetone:water (100:0)	101.19 \pm 6.33	486.73 \pm 30.44	6.25
Acetone:water (97.5:2.5)	98.86 \pm 10.44	475.51 \pm 50.20	10.56
Acetone:water (95:5)	98.47 \pm 3.34	473.64 \pm 16.06	3.39
Acetone:water (92.5:7.5)	98.10 \pm 6.31	471.85 \pm 30.36	6.43
Acetone:water (90:10)	100.92 \pm 7.74	485.44 \pm 37.22	7.67
Acetone:water (85:15)	91.39 \pm 4.87	439.60 \pm 23.43	5.33
Acetone:water (80:20)	101.81 \pm 6.51	489.71 \pm 31.32	6.39
Acetone:water (75:25)	93.80 \pm 16.32	451.20 \pm 78.49	17.40

Table 5

Recovered dose (RD), emitted dose (ED), fine particle fraction (FPF), recovery and emission of salbutamol sulphate from formulations containing mannitol which was crystallised using anti-solvents containing different acetone:water ratios (values are the mean \pm standard deviation, $n = 3$).

Formulation	RD (μg)	ED (μg)	Recovery (%)	Emission (%)	Impaction loss (%)	MMAD (μg)	GSD (μm)	FPF (%)
Commercial mannitol	381.53 \pm 8.27	367.30 \pm 8.81	79.32 \pm 1.72	96.28 \pm 0.22	75.65 \pm 0.73	3.04 \pm 0.16	2.16 \pm 0.01	15.42 \pm 1.14
Mannitol crystallised using: acetone:water (100:0)	426.60 \pm 25.32	396.69 \pm 20.89	88.69 \pm 5.26	92.93 \pm 1.56	38.05 \pm 1.97	3.18 \pm 0.11	2.14 \pm 0.02	41.52 \pm 2.61
Acetone:water (97.5:2.5)	439.21 \pm 34.25	409.73 \pm 28.68	91.31 \pm 7.12	93.33 \pm 0.90	34.79 \pm 1.51	3.27 \pm 0.09	2.15 \pm 0.01	43.19 \pm 0.66
Acetone:water (95:5)	458.73 \pm 74.07	433.32 \pm 69.07	95.37 \pm 15.40	94.48 \pm 0.57	35.47 \pm 3.78	3.14 \pm 0.06	2.17 \pm 0.02	43.99 \pm 2.62
Acetone:water (92.5:7.5)	422.39 \pm 70.64	400.43 \pm 70.57	87.82 \pm 14.68	94.70 \pm 0.96	38.45 \pm 2.26	2.88 \pm 0.22	2.35 \pm 0.23	42.88 \pm 1.30
Acetone:water (90:10)	455.49 \pm 32.50	432.28 \pm 27.06	94.70 \pm 6.76	94.94 \pm 1.14	38.70 \pm 11.60	3.14 \pm 0.01	2.18 \pm 0.06	41.65 \pm 7.90
Acetone:water (85:15)	395.21 \pm 95.44	373.21 \pm 101.27	82.16 \pm 19.84	93.90 \pm 3.29	48.29 \pm 8.04	3.19 \pm 0.11	2.16 \pm 0.02	33.98 \pm 5.34
Acetone:water (80:20)	441.56 \pm 20.74	414.46 \pm 20.99	91.80 \pm 4.31	93.85 \pm 0.73	39.75 \pm 1.37	3.11 \pm 0.14	2.15 \pm 0.03	41.04 \pm 0.54
Acetone:water (75:25)	400.11 \pm 41.04	375.11 \pm 45.81	83.18 \pm 8.53	93.63 \pm 2.68	50.61 \pm 7.72	3.03 \pm 0.22	2.17 \pm 0.05	33.07 \pm 3.66

(Tables 1 and 6). The FPF of salbutamol obtained from the formulation containing commercial mannitol was $15.42 \pm 1.14\%$ while FPF obtained from powder blends containing crystallised mannitol ranged between $33.07 \pm 3.66\%$ and $43.99 \pm 2.62\%$ (Table 5). The FPF from all the crystallised mannitol formulations was higher ($P < 0.05$) than that from the formulation containing commercial mannitol, indicating an enhanced DPI performance for the former formulations. A higher FPF value indicates increased amounts of salbutamol sulphate deposited on the lower stages of the MSLI and concurrently lower amounts on the upper stages (MSLI stage 1). This typifies an improved aerosolisation performance, with the target site for salbutamol sulphate being primarily in the lower airways (Price and Clissold, 1989). Although, ANOVA test showed that the presence of water in crystallisation medium had significant effect on FPF of formulation blend, there were no significant differences between the FPF of drug delivered using formulations containing crystallised mannitol derived using anti-solvent containing 90–100% acetone ($P > 0.05$). Nevertheless, the highest FPF ($43.99 \pm 2.62\%$) was obtained from the formulation containing mannitol crystallised using acetone:water (95:5) and this was about three times higher than the FPF obtained using commercial grade mannitol ($15.42 \pm 1.14\%$).

The impaction loss of drug (i.e. the amount of salbutamol sulphate depositing in the IP and MSLI stage 1 expressed as the per-

centage of the recovered dose) from all the formulations containing crystallised mannitol was significantly less than that from blends containing commercial mannitol. For example, the impaction loss decreased from 75.65% from aerosolised powders containing commercial mannitol to $34.79 \pm 1.51\%$ for formulations containing mannitol derived using acetone:water (97.5:2.5) as anti-solvent (Table 5). Although, the impaction loss does appear to increase for formulations containing crystallised mannitol obtained using acetone containing large amounts of water (15–25%), the increase was not as high as the value obtained when commercial mannitol was incorporated into the formulation.

A similar MMAD for salbutamol sulphate was obtained from all formulations, which was probably anticipated given that the same batch of salbutamol was used for all formulation blends.

The percentage of salbutamol sulphate depositing on each stage of the MSLI from the formulation containing commercial mannitol was considerably different compared to the amounts obtained using crystallised mannitol formulation blends (Table 6). The amount of salbutamol sulphate removed by stage 1 of the MSLI when aerosolised using a commercial mannitol-containing blend was 72.95% of the RD and it is unlikely these particles would reach the lower part of the airways. The corresponding values from the blends containing crystallised mannitol varied between $21.65 \pm 4.20\%$ and $44.52 \pm 10.90\%$. Drug deposition on inhaler and

Table 6

Percentage of salbutamol sulphate deposited on different stages of MSLI and the Inhaler when aerosolised from different DPI formulations containing mannitol which was crystallised using anti-solvents containing different acetone:water ratios (all values are percentage of the recovered dose and are mean standard deviation, $n = 3$).

	I & M	IP	MSLI 1	MSLI2	MSLI3	MSLI4	MSLI5
Commercial mannitol	3.73 \pm 0.22	2.70 \pm 0.23	72.95 \pm 0.50	3.77 \pm 0.39	7.57 \pm 0.70	6.99 \pm 2.30	2.28 \pm 0.25
Mannitol crystallised using: acetone:water (100:0)	7.07 \pm 1.56	10.09 \pm 1.85	27.96 \pm 1.15	11.78 \pm 1.17	19.99 \pm 1.09	17.87 \pm 1.96	5.24 \pm 0.72
Acetone:water (97.5:2.5)	6.48 \pm 1.24	11.94 \pm 1.83	21.65 \pm 4.20	14.35 \pm 0.95	18.78 \pm 1.81	18.34 \pm 1.17	4.96 \pm 0.42
Acetone:water (95:5)	5.52 \pm 0.57	13.58 \pm 0.78	21.89 \pm 4.26	13.44 \pm 0.84	19.46 \pm 3.55	20.18 \pm 1.10	5.93 \pm 0.52
Acetone:water (92.5:7.5)	5.29 \pm 0.96	16.37 \pm 1.62	22.08 \pm 0.65	12.46 \pm 0.29	17.27 \pm 1.26	16.74 \pm 8.36	9.79 \pm 6.05
Acetone:water (90:10)	5.06 \pm 1.14	11.12 \pm 3.99	27.58 \pm 15.50	12.99 \pm 2.10	18.91 \pm 5.09	18.48 \pm 3.39	5.87 \pm 0.12
Acetone:water (85:15)	6.09 \pm 3.29	8.17 \pm 1.59	40.12 \pm 8.88	11.00 \pm 1.82	14.90 \pm 2.75	15.31 \pm 2.70	4.41 \pm 0.25
Acetone:water (80:20)	6.15 \pm 0.73	6.76 \pm 1.80	32.99 \pm 3.11	10.89 \pm 1.63	19.28 \pm 1.54	18.66 \pm 0.72	5.27 \pm 0.39
Acetone:water (75:25)	6.37 \pm 2.68	6.09 \pm 3.18	44.52 \pm 10.90	8.43 \pm 2.87	14.67 \pm 2.46	15.52 \pm 0.97	4.40 \pm 0.49

mouthpiece adaptor increased from 3.73% to 5.06–7.07% after aerosolisation of the formulations containing commercial and crystallised mannitol, respectively. Drug deposition on the IP was also higher from the latter formulations (Table 6). The amount of drug deposited on stages 2–5 from blends containing crystallised mannitol was larger than that obtained from the commercial mannitol-containing formulations (Table 6).

The enhancement in the aerosolisation performance achieved using the formulations containing crystallised mannitol could be accounted for by weaker adhesive forces acting between salbutamol sulphate particles and crystallised mannitol particles, due to the elongated shape of the latter. It is known that particle shape has a significant influence on particle adhesion (Zeng et al., 2001) and needle-shaped crystals have more ability to stay airborne in air-flow than isometric particles with the same geometric size (Fulfs et al., 1997). The elongated shape of the crystallised mannitol reduces the effective drug-carrier contact area and as a result of the higher inter-particulate distances then the van der Waals attractive forces will be decreased. The needle-shaped particles have somewhat planar surfaces and their cohesive interactions is generally expected to be larger than spherical particles, therefore, the higher powder cohesiveness for needle-shaped crystals is expected to negatively affect powder fluidisation (powder dispersion) and this is evident from Table 6 showing higher amounts of drug deposited on inhaler and mouthpiece adaptor, and induction port due to high cohesiveness of the needle-shaped carrier compared to commercial mannitol (less cohesive). On the other hand, data reported in Table 6 showed that higher powder cohesiveness for needle-shaped crystals was not a limiting factor for powder re-dispersion (drug detachment from carrier) as better aerosolisation performance was obtained for formulation blends containing needle-shaped carrier.

Another factor can affect DPI performance is the presence of fine carrier particles adhered to surfaces of large carrier particles (Islam et al., 2004). It has been shown that FPF and dispersion of salbutamol sulphate increased when fine lactose particles were included in blends containing coarser lactose particles (Zeng et al., 1998; Louey and Stewart, 2002). The particle size distribution indicated that despite sieving (63–90 μm) crystallised mannitol particles contained a proportion of fine carrier particles, as evident from SEM images (Figs. 2 and 3). The amount of fine particles adhered to the crystallised carrier particles appeared to be greater than in the commercial mannitol sample, which could have promoted the aerosolisation performance of the resulted formulation blends. Interestingly, the resultant FPF obtained from the crystallised mannitol formulations was a linear function of percentage of fine particles < 10.50 μm in the corresponded sieved crystallised mannitol carrier ($r^2 = 0.8475$; Fig. 5a).

A linear relationship was also established between the surface-volume mean diameter of the crystallised mannitol and FPF produced after aerosolisation of the corresponding formulation (Fig. 5b). The needle-shape mannitol crystals have a higher surface-volume mean diameter compared to rounded particles.

A lower FPF of salbutamol sulphate was obtained from formulations containing mannitol crystallised using acetone:water mixture containing 15% and 25% water than from powders containing mannitol crystallised from acetone:water mixtures (100:0–90:10). The higher elongation ratio of the latter particles may lead to a lower aerodynamic diameter and hence a greater penetration of the mannitol deeper into the MSLI. The mannitol carrier particles crystallised using the higher proportion of water in the anti-solvent media contained rounder particles, with short needles adherent to the surface (Fig. 1g–i). The shape of the particles obtained at high water concentrations were more similar to that of the commercial grade mannitol compared to the mannitol obtained using anti-solvent containing lower amounts of water (Figs. 1a–2i). Thus, mannitol particles crystallised using acetone containing high

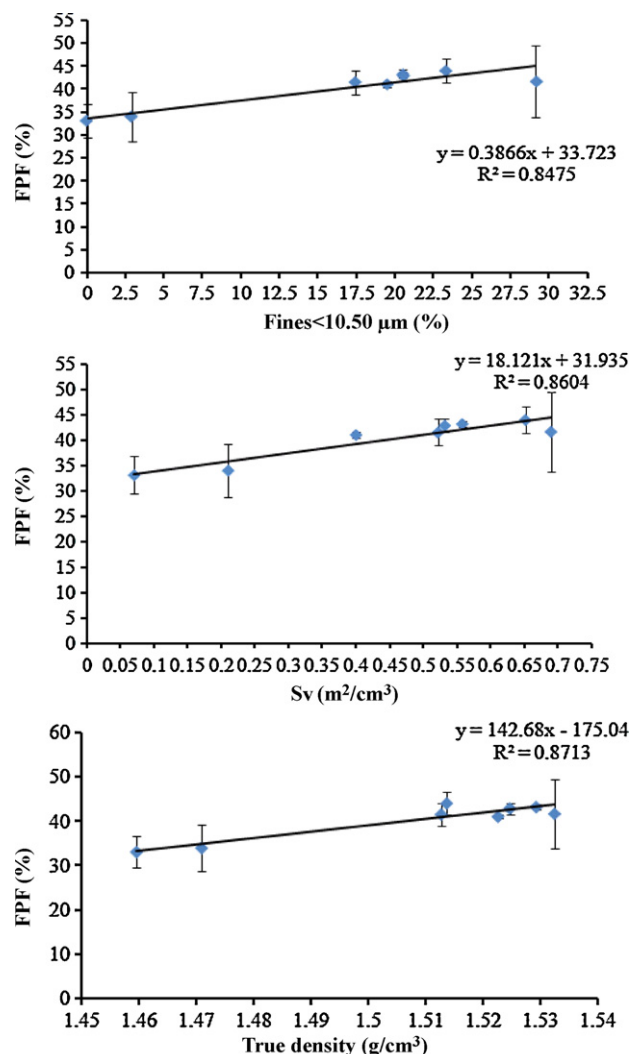


Fig. 5. The effect of formulation factors on the fine particle fraction (FPF) of salbutamol sulphate (mean \pm standard deviation, $n = 3$).

amount of water (from 15% to 25%) indicated that some of the needle-shaped particles present were aggregated, whereas mannitol crystallised derived using acetone containing 0–15% water were homogeneously dispersed (Fig. 1). This was also confirmed by particle size distribution data showing bimodal or multimodal patterns for the samples obtained using acetone containing 15–25% water (figures not shown). The larger carrier particles present in the latter samples may be responsible for lower DPI performance as such particles exhibit higher frictional and press-on forces, resulting in higher drug-carrier adhesive forces in the formulation (Dickhoff et al., 2003, 2005). The lower percentage of fine carrier particles and smaller S_v (surface area based on volume distribution) of the mannitol particles produced using acetone:water (85:15–75:25) anti-solvent also contributes to the lower FPF (Fig. 5a). The true density of carrier may also affect the performance of DPI formulations, since a linear relationship was found to exist between FPF from the test formulations and test carrier true density ($r^2 = 0.8713$; Fig. 5c). A linear relationship ($r^2 = 0.8604$) could be established between S_v values of mannitol samples and FPF. This indicates that S_v of the carrier has a significant effect on aerosolisation performance of DPI formulations (Fig. 5b) and generally carrier with higher S_v values showed better performance than of carrier particles with lower S_v value.

4. Conclusions

Crystallisation of mannitol particles using different ratios of acetone:water resulted in particles with different physicochemical properties in comparison to those present in commercial grade mannitol. All the crystallised samples showed a higher compressibility index, lower particle size with higher size distribution polydispersity, higher amounts of fines, higher volume specific surface area, and lower bulk and tapped density. The particle morphology of the commercial mannitol particles was rounded and the topology of the surface contained ridges. Mannitol particles crystallised from acetone:water in contrast were elongated with smooth surfaces. Like commercial mannitol, crystallised mannitol samples using water percentages >10% comprised the β form; while crystallised mannitol samples using water percentages <10% comprised the α form. The efficiency of dispersion of salbutamol sulphate from powders containing crystallised mannitol was dependent upon the proportion of water present in the anti-solvent used in the crystallisation procedure. All crystallised mannitol formulations resulted in lower uniformity. Best dispersion was obtained when the water content was 15% or less. Nevertheless the dispersion was better from all of the crystallised mannitol-containing powders than from formulations containing commercial mannitol. A linear relationship was found between the amount of fine carrier particles in the blends, carrier true density, carrier surface-volume mean diameter, carrier volume specific surface area and FPF of formulation blends. Clearly despite the inherent poor flow properties of such crystals, the use of formulations needle-shaped particles of carrier and/or drug requires further investigation.

Acknowledgements

Waseem Kaialy thanks the University of Damascus for providing PhD scholarship. The authors thank Ian Slipper, School of Science, University of Greenwich for taking SEM images.

References

- Bosquillon, C., Lombry, C., Pr at, V., Vanbever, R., 2001. Influence of formulation excipients and physical characteristics of inhalation dry powders on their aerosolization performance. *J. Control. Release* 70, 329–339.
- Burger, A., Henck, J.O., Hetz, S., Rollinger, J.M., Weissnicht, A.A., Stottner, H., 2000. Energy/temperature diagram and compression behavior of the polymorphs of D-mannitol. *J. Pharm. Sci.* 89, 457–468.
- Byron, P.R., Kelly, E.L., Kontny, M.J., Lovering, E.G., Poochikian, G.K., Sethi, S., 1994. Recommendations of the USP advisory panel on aerosols on the USP general chapters on aerosols (601) and uniformity of dosage units (905). *Pharm. Forum*, 7477–7503.
- Campbell, R.S.N., Williams, A.C., Grimsey, I.M., Booth, S.W., 2002. Quantitative analysis of mannitol polymorphs. X-ray powder diffractometry—exploring preferred orientation effects. *J. Pharm. Biomed. Anal.* 28, 1149–1159.
- Carr, R.L., 1965a. Evaluating flow properties of solids. *Chem. Eng.* 72, 163–168.
- Carr, R.L., 1965b. Classifying flow properties of solids. *Chem. Eng.* 72, 169–172.
- Chan, H.K., Chew, N.Y.K., 2003. Novel alternative methods for the delivery of drugs for the treatment of asthma. *Adv. Drug Deliv. Rev.* 55, 793–805.
- Dickhoff, B.H.J., de Boer, A.H., Lambregts, D., Frijlink, H.W., 2005. The interaction between carrier rugosity and carrier payload, and its effect on drug particle redispersion from adhesive mixtures during inhalation. *Eur. J. Pharm. Sci.* 59, 197–205.
- Dickhoff, B.H.J., de Boer, A.H., Lambregts, D., Frijlink, H.W., 2003. The effect of carrier surface and bulk properties on drug particle detachment from crystalline lactose carrier particles during inhalation, as function of carrier payload and mixing time. *Eur. J. Pharm. Sci.* 56, 291–302.
- European Commission—Health & Consumer Protection Directorate, 2002. Provisional Statement on the Safety of Calf-derived Rennet for the Manufacture of Pharmaceutical Grade Lactose.
- Fults, K.A., Miller, I.F., Hickey, A.J., 1997. Effect of particle morphology on emitted dose of fatty acid-treated disodium cromoglycate powder aerosols. *Pharm. Dev. Technol.* 2, 67–79.
- Islam, N., Stewart, P., Larson, I., Hartley, P., 2004. Lactose surface modification by decantation: are drug-fine lactose ratios the key to better dispersion of salmeterol xinafoate from lactose-interactive mixtures? *Pharm. Res.* 21, 492–499.
- Larhrib, H., Martin, G.P., Marriott, C., Prime, D., 2003. The influence of carrier and drug morphology on drug delivery from dry powder formulations. *Int. J. Pharm.* 257, 283–296.
- Louey, M.D., Stewart, P.J., 2002. Particle interactions involved in aerosol dispersion of ternary interactive mixtures. *Pharm. Res.* 19, 1524–1531.
- Maa, Y.F., Prestrelski, S.J., 2000. Biopharmaceutical powders particle formation and formulation considerations. *Curr. Pharm. Biotechnol.* 1, 283–302.
- Price, A.H., Clissold, S.P., 1989. Salbutamol in the 1980s. A reappraisal of its clinical efficacy. *Drugs* 38, 77–122.
- Pritchard, J.N., 2001. The influence of lung deposition on clinical response. *J. Aerosol Med.* 14, 19–26.
- Rabbani, N.R., Seville, P.C., 2005. The influence of formulation components on the aerosolisation properties of spray-dried powders. *J. Control. Release* 110, 130–140.
- Rowe, R.C., Sheskey, P.J., Weller, P.J., 2003. *Handbook of Pharmaceutical Excipients*. Pharmaceutical Press, London, UK.
- Saint-Lorant, G., Leterme, P., Gayot, A., Flament, M.P., 2007. Influence of carrier on the performance of dry powder inhalers. *Int. J. Pharm.* 334, 85–91.
- Smyth, H.D.C., Hickey, A.J., 2005. Carriers in drug powder delivery. Implications for inhalation system design. *Am. J. Drug Deliv.* 3, 117–132.
- Srichana, T., Martin, G.P., Marriott, C., 1998. Dry powder inhalers: the influence of device resistance and powder formulation on drug and lactose deposition in vitro. *Eur. J. Pharm. Sci.* 7, 73–80.
- Steckel, H., Bolzen, N., 2004. Alternative sugars as potential carriers for dry powder inhalations. *Int. J. Pharm.* 270, 297–306.
- Tee, S.K., Marriott, C., Zeng, X.M., Martin, G.P., 2000. The use of different sugars as fine and coarse carriers for aerosolised salbutamol sulphate. *Int. J. Pharm.* 208, 111–123.
- Timsina, M.P., Martin, G.P., Marriott, C., Ganderton, D., Yainneskis, M., 1994. Drug delivery to the respiratory tract using dry powder inhalers. *Int. J. Pharm.* 101, 1–13.
- USP Pharmacopeia, 2003. The Official Compendia of Standards, USP 26/NF 21. United States Pharmacopeial Conventio, Inc, Rockville, MD, Aerosols <601>, pp. 2114–2123.
- Walter-Levy, L., 1968. Cristallochimie-sur les vari t s cristallines du D-mannitol. *C.R. Acad. Sci. Paris Ser.* 267, 1779–1782.
- Yoshinari, T., Forbes, R.T., York, P., Kawashima, Y., 2002. Moisture induced polymorphic transition of mannitol and its morphological transformation. *Int. J. Pharm.* 247, 69–77.
- Zeng, X.M., Martin, G.P., Marriott, C., Pritchard, J., 2001. Lactose as a carrier in dry powder formulations. The influence of surface characteristics on drug delivery. *J. Pharm. Sci.* 90, 1424–1434.
- Zeng, X.M., Martin, G.P., Tee, S.K., Marriott, C., 1998. The role of fine particle lactose on the dispersion and deaggregation of salbutamol sulphate in an air stream in vitro. *Int. J. Pharm.* 176, 99–110.